

Strong coupling and stimulated emission in single parabolic quantum well microcavity for terahertz cascade

A. Tzimis, A. V. Trifonov, G. Christmann, S. I. Tsintzos, Z. Hatzopoulos, I. V. Ignatiev, A. V. Kavokin, and P. G. Savvidis

Citation: *Applied Physics Letters* **107**, 101101 (2015); doi: 10.1063/1.4930165

View online: <http://dx.doi.org/10.1063/1.4930165>

View Table of Contents: <http://scitation.aip.org/content/aip/journal/apl/107/10?ver=pdfcov>

Published by the AIP Publishing

Articles you may be interested in

[Strong coupling at room temperature in ultracompact flexible metallic microcavities](#)

Appl. Phys. Lett. **102**, 011118 (2013); 10.1063/1.4773881

[Dynamical Franz–Keldysh effect in GaAs/AlGaAs multiple quantum wells induced by single-cycle terahertz pulses](#)

Appl. Phys. Lett. **97**, 211902 (2010); 10.1063/1.3518483

[Strong enhancement of terahertz response in GaAs/AlGaAs quantum well photodetector by magnetic field](#)

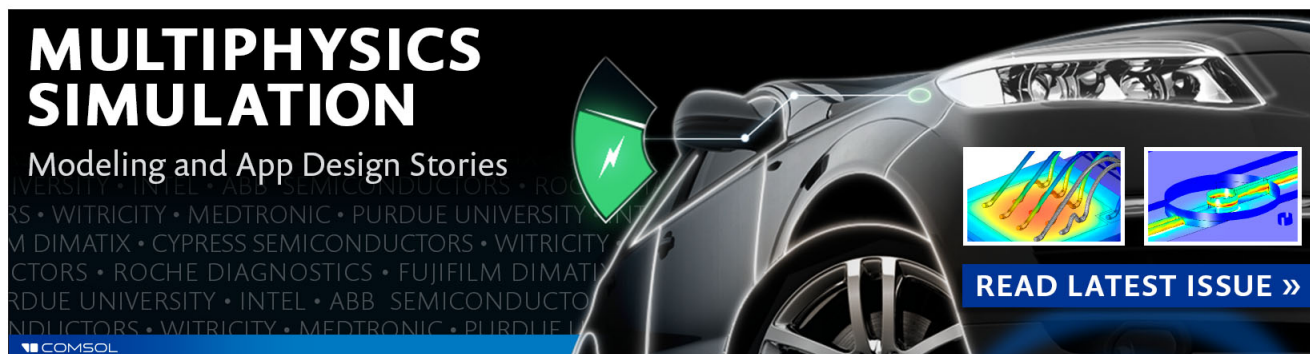
Appl. Phys. Lett. **97**, 022102 (2010); 10.1063/1.3462300

[Enhanced terahertz emission from coherent longitudinal optical phonons in a quantum well structure under applied bias](#)

Appl. Phys. Lett. **94**, 171105 (2009); 10.1063/1.3126446

[Effect of spatial nonlocality on terahertz optical interaction with quantum wells](#)

J. Appl. Phys. **105**, 073515 (2009); 10.1063/1.3103776

The advertisement features a dark background with a high-tech car on the right. On the left, the text 'MULTIPHYSICS SIMULATION' is in large, bold, white letters. Below it, 'Modeling and App Design Stories' is in a smaller white font. A green shield with a white lightning bolt is positioned between the text and the car. On the right, two small inset images show simulation results: one with a color-coded stress or temperature distribution on a mechanical part, and another showing a blue and yellow wave pattern. At the bottom right, a blue button with white text says 'READ LATEST ISSUE >>'. The COMSOL logo is in the bottom left corner.

**MULTIPHYSICS
SIMULATION**

Modeling and App Design Stories

UNIVERSITY • INTEL • ABB SEMICONDUCTORS • ROCH
RS • WITRICITY • MEDTRONIC • PURDUE UNIVERSITY • IN
M DIMATIX • CYPRESS SEMICONDUCTORS • WITRICITY
CTORS • ROCHE DIAGNOSTICS • FUJIFILM DIMATI
RDUE UNIVERSITY • INTEL • ABB SEMICONDUCTO
NDUCTORS • WITRICITY • MEDTRONIC • PURDUE U

COMSOL

READ LATEST ISSUE >>

Strong coupling and stimulated emission in single parabolic quantum well microcavity for terahertz cascade

A. Tzimis,^{1,2} A. V. Trifonov,³ G. Christmann,² S. I. Tsintzos,² Z. Hatzopoulos,^{2,4}
 I. V. Ignatiev,³ A. V. Kavokin,^{3,5} and P. G. Savvidis^{1,2}

¹*Department of Materials Science and Technology, University of Crete, 71003 Heraklion, Crete, Greece*

²*Institute of Electronic Structure and Laser, Foundation for Research and Technology - Hellas, 71110 Heraklion, Crete, Greece*

³*Spin Optics Laboratory, State University of Saint-Petersburg, 1 Ulianovskaya, 198504 St. Petersburg, Russia*

⁴*Department of Physics, University of Crete, 71003 Heraklion, Crete, Greece*

⁵*School of Physics and Astronomy, University of Southampton, Southampton SO17 1BJ, United Kingdom*

(Received 15 June 2015; accepted 25 August 2015; published online 8 September 2015)

We report observation of strong light-matter coupling in an AlGaAs microcavity (MC) with an embedded single parabolic quantum well. The parabolic potential is achieved by varying aluminum concentration along the growth direction providing equally spaced energy levels, as confirmed by Brewster angle reflectivity from a reference sample without MC. It acts as an active region of the structure which potentially allows cascaded emission of terahertz (THz) light. Spectrally and time resolved pump-probe spectroscopy reveals characteristic quantum beats whose frequencies range from 0.9 to 4.5 THz, corresponding to energy separation between relevant excitonic levels. The structure exhibits strong stimulated nonlinear emission with simultaneous transition to weak coupling regime. The present study highlights the potential of such devices for creating cascaded relaxation of bosons, which could be utilized for THz emission. © 2015 AIP Publishing LLC.

[<http://dx.doi.org/10.1063/1.4930165>]

The terahertz (THz) spectral region (~ 0.3 to 10 THz) remains one of the most unexploited parts of the electromagnetic spectrum, despite its potential applications in various fields such as medicine, biosensing, and industrial inspection. The main reason has been the lack of reliable and efficient radiation sources, which makes the development of such emitters a technological challenge of high importance. This is mainly due to the fact that direct generation of THz radiation is limited by the lack of materials with appropriately small bandgap. A great achievement towards this direction is the development of quantum cascade laser (QCL) demonstrated in 1994 with a frequency of 75 THz.¹ Contrary to typical semiconductor lasers which use interband transitions to emit light, QCLs use intersubband transitions which nowadays are able to produce light with even lower frequency, typically in the 1 to 5 THz range.^{2,3} To combine strong optical gain and carrier transport through the device, a complex band structure is required, particularly because the active region is repeated several times.⁴

Alternative ways for the emission of THz photons using microcavity systems in the strong coupling regime (SCR)^{5–11} have been recently proposed.^{12–14} Such devices are based on the strong coupling between light (photons in a cavity) and matter (excitons in semiconductor quantum wells) forming new quasiparticles called polaritons. Theoretical proposals describe the production of THz emission from the transition between the upper and the lower polariton state¹² and the use of the oscillation of the dipole moment of polaritons from coupled quantum wells.¹³ Of particular interest is a recent theoretical proposal of a bosonic cascade laser using the equally spaced excitonic levels of a parabolic quantum well (PQW).¹⁴ In polaritonic structures, the possibility to have a macroscopically occupied ground state is expected to enhance the

transitions to the ground state (through bosonic stimulation) and thus improve THz emission. Therefore, the study of semiconductor microcavities utilizing PQW capable of supporting stimulated cascaded relaxation between equidistant energy levels for THz emission is imminent.

This letter reports on the SCR in a microcavity containing a PQW.^{12,14–17} When the PQW is studied alone,¹⁸ the expected equally spaced excitonic transitions are observed. When placed in a microcavity, the full structure exhibits a clear anticrossing between the ground state heavy hole (hh)/light hole (lh) excitons and the cavity mode, revealing the SCR. The study of the excitonic relaxation shows oscillations with frequencies in the THz range. Furthermore, under nonresonant optical excitation, the microcavity exhibits stimulated emission in the weak coupling regime. This is a necessary prerequisite for a cascaded bosonic relaxation which will result in THz emission.

Both samples under study were grown by molecular-beam epitaxy on n^+ GaAs substrate with n^+ GaAs buffer layer and a GaAs cap layer on the top to prevent them from oxidation. The first one is a single PQW whose profile was grown by varying the aluminum concentration of $\text{Al}_x\text{Ga}_{1-x}\text{As}$, producing a 50 nm quantum well at the top of potential profile with its band structure reported in Fig. 1(a). The parabolic potential is broken into several linear growth segments, and the aluminum concentration is adjusted continuously during growth. The structure was designed to provide a reasonable number ($\simeq 15$) of equally spaced excitonic energy levels which include both hh and lh excitonic transitions. All allowed transitions are shown with arrows in Fig. 1(a). In the second sample, a similar PQW was embedded inside a microcavity. A λ cavity layer was sandwiched between two $\text{Al}_{0.15}\text{Ga}_{0.85}\text{As}/\text{AlAs}$ distributed Bragg reflectors (DBRs) with 22 pairs for the bottom one and

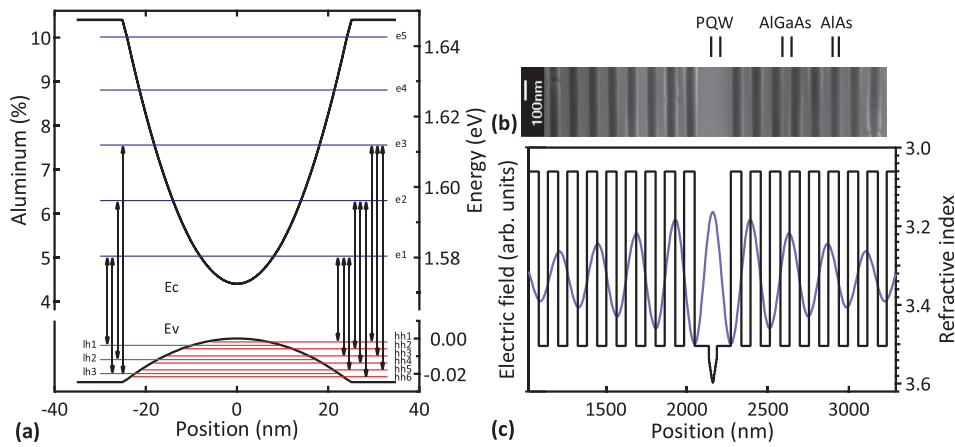


FIG. 1. (a) The designed parabolic quantum well composition profile (Al \approx 4.5%–10.5%), calculated valence (Ev) and conduction (Ec) bands, electron (e), heavy hole (hh), and light hole (lh) energy levels with the allowed transitions (vertical arrows). (b) SEM image of the central region of the microcavity and (c) the corresponding simulation of the electric field along the structure and the refractive index distribution inside the microcavity.

17 for the top one. The PQW was inserted at the center of the $\text{Al}_{0.15}\text{Ga}_{0.85}\text{As}$ cavity layer at the antinode of the electric field to maximize the light-matter coupling. Fig. 1(b) is a SEM image which shows the central region of the microcavity, while Fig. 1(c) is the calculated electric field along that part of the structure.

We first assess the quality of the PQW by measuring the different excitonic levels, at 28 K, in the structure without microcavity. Brewster angle reflectivity was employed to probe these transitions due to its high signal to noise ratio. At the Brewster angle, the reflection from the surface of the sample is greatly reduced and, consequently, the sensitivity to the refractive index modulations caused by the excitonic resonances is increased. In our setup, light from a halogen lamp passes through a polariser to acquire transverse magnetic (TM) polarisation, a lens is used to focus the light on the sample and a mirror to guide it on the specific Brewster angle ($\approx 74^\circ$). The reflectivity is collected and sent to a spectrometer coupled to a liquid-nitrogen-cooled charged coupled device (CCD).

Fig. 2(a) shows the Brewster angle reflectivity spectrum of the PQW (right side of the graph). Both hh and lh excitons from the fundamental transition can be seen with a 2.6 meV splitting. At higher energies, smaller spectral features that we attribute to specific excitonic transitions are visible, noted with the respective numbers. The electron-hole energy levels were calculated by solving the Schrodinger equation while the binding energies were computed by the variational method.^{19,20} Some transitions are not clearly noticeable due to their lower oscillator strength. The extracted energy positions of all observed states are plotted in the inset graph showing the expected equally spaced optical transitions with energy separation of ~ 4.3 meV. These equally spaced energy levels are characteristic of harmonic confinement proving the successful realisation of the parabolic profile and potentially allow the bosonic cascade THz emission recently proposed.¹⁴ The area of the circular markers (log scale) is proportional to the calculated oscillator strength of the excitonic levels. Good agreement between measured reflectivity dips and calculated oscillator strengths is found. Potential discrepancies could result from deviations from the parabolic potential of the fabricated quantum well which could slightly modify the energy positions of some of the excited states.

In order to reveal the potential of the PQW for THz generation, we study the dynamics of excitonic relaxation by using pump-probe spectroscopy. In our setup, the 80-fs

pulses from a Ti:Sapphire laser are used for the pump and probe beams. The reflectivity of the probe beam is measured at normal incidence geometry, by using a monochromator

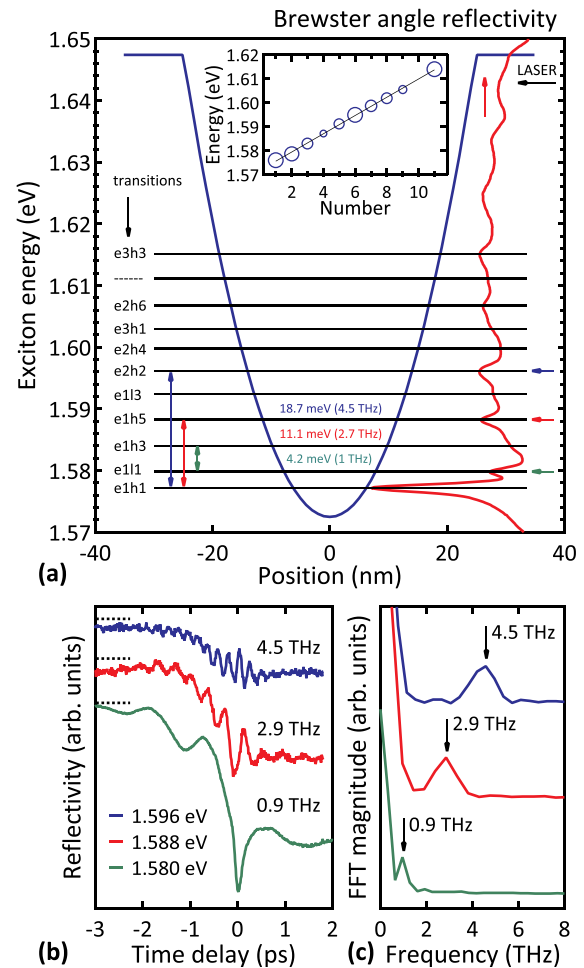


FIG. 2. (a) Potential profile in the parabolic quantum well (blue line) and reflectivity spectrum in Brewster angle configuration (red line, right side), horizontal black lines show the excitonic energy levels. (a) Inset) Energy position of the excitonic transitions (open circles) along with a linear fit (black line). The area of the circles (log scale) is proportional to the corresponding oscillator strength of each excitonic level. (b) Pump-probe reflectivity measurements in three different detection energies, which are shown in (a) with horizontal colored arrows, demonstrating the quantum beats of different excitonic states, which are shown in (a) with vertical colored arrows. The colored numbers in (a) are the energy (frequency) distances between the interfering states obtained from the reflectivity spectrum. Time traces were vertically spaced for clarity and zero baselines are shown with horizontal dashed lines. (c) The Fast Fourier Transform of the time traces.

with a photodiode connected to a lock-in amplifier. This spectral selection allowed us to detect signal for different excitonic transition as a function of delay between the pump and probe pulses.

Fig. 2(b) shows the pump-probe reflectivity measurements for three different detection energies. These show pronounced oscillations, which we interpret as quantum beats between the 1st and 6th, 1st and 4th, and 2nd and 3rd excitonic levels. The frequencies of oscillations (extracted by Fast Fourier Transform shown in Fig. 2(c)) are in the THz range, 4.5 THz, 2.9 THz, and 0.9 THz, corresponding to energy separation of 18.6 meV, 12 meV, and 3.7 meV, respectively. Vertical arrows of corresponding colors in Fig. 2(a) show the excitonic levels which contribute to the quantum beats. These data demonstrate that excitons occupying different quantum confined states in PQW maintain mutual coherence for a few picoseconds, defined by the decay time due to inhomogeneous broadening of the excitonic states in the structure under study. We note here, that any remaining background in Fig. 2(b) is due to the long-lived excitonic reservoir states which have typical lifetimes of several nanoseconds.²¹

We now study the possibility of achieving the SCR with such a PQW embedded in a microcavity. For that, we characterized our microcavity sample at 28 K using a photoluminescence imaging setup. The sample is excited with a tuneable continuous-wave Ti:Sapphire laser, at a wavelength corresponding to the first minimum of the DBR reflectivity on the high energy side of the spectrum (753 nm), just below AlGaAs barrier absorption, to directly inject carriers in the PQW. Laser light is focused through an objective lens and the emission at the Fourier plane is imaged on the entrance slit of an imaging spectrometer coupled to a liquid-nitrogen-cooled CCD.

Fig. 3 shows the measured energy versus angle photoluminescence image of the sample. A strong emission peak

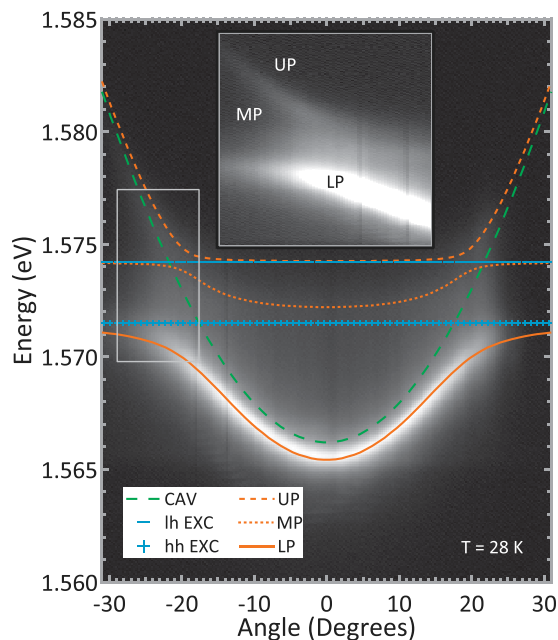


FIG. 3. Energy versus angle photoluminescence image and dispersion fittings obtained from the solutions of a 3×3 coupled harmonic Hamiltonian. Heavy hole (hh) and light hole (lh) excitons (horizontal plus and minus symbols, respectively). Polariton branches, upper (dashed line), middle (dots), and lower (continuous line). Cavity mode (parabolic dashed line).

exhibiting the characteristic dispersion of a lower polariton (LP) branch is clearly visible. By saturating the color scale, it is possible to observe two extra polariton branches, the middle (MP) one and the upper (UP) one (Fig. 3 inset). These three branches reveal the SCR involving both the hh and lh excitons. The fitted polariton branches were extracted by a 3×3 coupled harmonic oscillator model,^{22,23} and the characteristic anticrossing behaviour of the SCR is observed. The hh-lh energy splitting is 2.7 meV, which is in good agreement with the reflectivity measurement on the bare PQW.

To examine the nonlinear emission characteristics of this PQW microcavity, we measure power dependent photoluminescence under excitation at the reflectivity dip at the edge of the DBR stop-band and tuned just below AlGaAs barrier energy to avoid unnecessary absorption. The measured normal incidence photoluminescence spectra with increasing excitation power, taken for optimal exciton-photon detuning, are plotted in Fig. 4(a). It shows an initially linear emission with increasing blueshift (Fig. 4(c)). At higher powers, nonlinear stimulated emission is observed with simultaneous line narrowing, plotted in Fig. 4(b), and collapse of SCR. Further evidence for stimulated relaxation is obtained from two-pump time-resolved experiments,²⁴ which show strong enhancement of the photoluminescence spectrum just below threshold for small time delays. The collapse of the SCR is observed from the position of lasing emission peak which coincides with the modelled bare cavity mode energy obtained from the fit to the polariton dispersions (Fig. 4(a)). Here, we note that although the observed nonlinear emission is not achieved in the SCR, nevertheless, it is a potential sign of bosonically enhanced relaxation in this system which could be utilized for THz emission as proposed.¹⁴ However, deterministic answer requires further experiments and is a subject of ongoing investigation. The

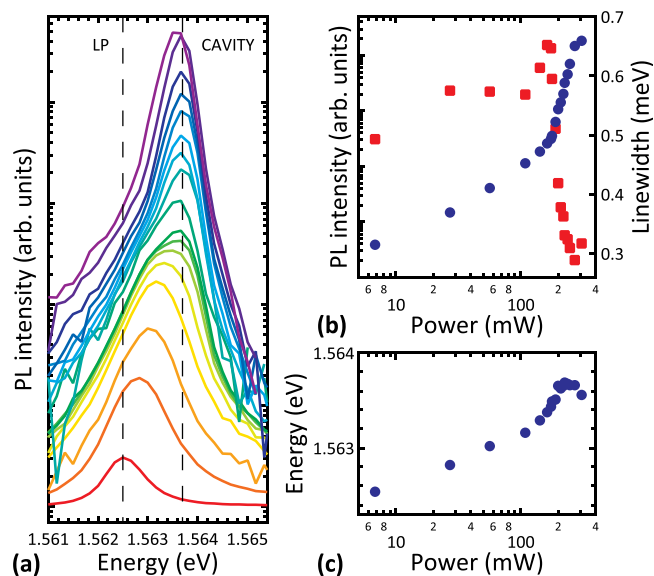


FIG. 4. (a) Photoluminescence spectra at normal incidence to the sample for an increasing power. (b) The integrated photoluminescence (circles) along with the linewidths (squares) versus power and (c) the corresponding peak positions.

dispersion of Fig. 3 and the power dependence of Fig. 4 were performed at different exciton-photon detuning conditions.

In conclusion, we observe the SCR in a microcavity using a PQW and identify coherent THz oscillations between different excitonic levels. Furthermore, strong nonlinear emission evidences stimulated relaxation and excitonic cascade in our system. Such cascaded relaxation, when accompanied with THz photon emission not shown here, could potentially lead to the development of QCL-type devices, which will require no population inversion and no application of external electric fields.

The authors acknowledge financial support from FP7 IRSES POLATER exchange grant, Greek GSRT ARISTEIA program Apollo, and the RFBR Grant No. 15-59-30406 PT. The work of A.V.K. was supported by the Russian Ministry of Education and Science (Contract No. 11.G34.31.0067), and the EPSRC Established Career Fellowship. The work of I.V.I. was supported by the SPbSU Grant No. 11.38.213.2014.

- ¹J. Faist, F. Capasso, D. L. Sivco, C. Sirtori, A. L. Hutchinson, and A. Y. Cho, *Science* **264**, 553 (1994).
- ²G. Scalari, C. Walther, J. Faist, H. Beere, and D. Ritchie, *Appl. Phys. Lett.* **88**, 141102 (2006).
- ³A. W. M. Lee, Q. Qin, S. Humar, B. S. Williams, Q. Hu, and J. L. Reno, *Appl. Phys. Lett.* **89**, 141125 (2006).
- ⁴B. S. Williams, *Nature Photon.* **1**, 517 (2007).
- ⁵C. Weisbuch, M. Nishioka, A. Ishikawa, and Y. Arakawa, *Phys. Rev. Lett.* **69**, 3314 (1992).
- ⁶A. Wallraff, D. Schuster, A. Blais, L. Frunzio, R. Huang, J. Majer, S. Kumar, S. Girvin, and R. Schoelkopf, *Nature* **431**, 162 (2004).
- ⁷E. Peter, P. Senellart, D. Martrou, A. Lemaître, J. Hours, J. M. Gerard, and J. Bloch, *Phys. Rev. Lett.* **95**, 067401 (2005).

- ⁸K. Hennessy, A. Badolato, M. Winger, D. Gerace, M. Atature, S. Gulde, S. Fält, E. L. Hu, and A. Imamoglu, *Nature* **445**, 896 (2007).
- ⁹D. Dini, R. Kohler, A. Tredicucci, G. Biasiol, and L. Sorba, *Phys. Rev. Lett.* **90**, 116401 (2003).
- ¹⁰M. Geiser, C. Walther, G. Scalari, M. Beck, M. Fischer, L. Nevou, and J. Faist, *Appl. Phys. Lett.* **97**, 191107 (2010).
- ¹¹Y. Todorov, A. M. Andrews, I. Sagnes, R. Colombelli, P. Klang, G. Strasser, and C. Sirtori, *Phys. Rev. Lett.* **102**, 186402 (2009).
- ¹²K. V. Kavokin, M. A. Kaliteevski, R. A. Abram, A. V. Kavokin, S. Sharkova, and I. A. Shelykh, *Appl. Phys. Lett.* **97**, 201111 (2010).
- ¹³O. Kyriienko, A. V. Kavokin, and I. A. Shelykh, *Phys. Rev. Lett.* **111**, 176401 (2013).
- ¹⁴T. C. H. Liew, M. M. Glazov, K. V. Kavokin, I. A. Shelykh, M. A. Kaliteevski, and A. V. Kavokin, *Phys. Rev. Lett.* **110**, 047402 (2013).
- ¹⁵M. Geiser, F. Castellano, G. Scalari, M. Beck, L. Nevou, and J. Faist, *Phys. Rev. Lett.* **108**, 106402 (2012).
- ¹⁶R. Colombelli, C. Ciuti, Y. Chassagneux, and C. Sirtori, *Semicond. Sci. Technol.* **20**, 985 (2005).
- ¹⁷M. Sundaram, A. Gossard, J. English, and R. Westervelt, *Superlattices Microstruct.* **4**, 683 (1988).
- ¹⁸R. C. Miller, A. C. Gossard, D. A. Kleinman, and O. Munteanu, *Phys. Rev. B* **29**, 3740 (1984).
- ¹⁹D. A. B. Miller, D. S. Chemla, T. C. Damen, A. C. Gossard, W. Wiegmann, T. H. Wood, and C. A. Burrus, *Phys. Rev. B* **32**, 1043 (1985).
- ²⁰A. V. Kavokin, J. J. Baumberg, G. Malpuech, and F. P. Laussy, *Microcavities* (Oxford University Press, 2009).
- ²¹A. V. Trifonov, S. N. Korotan, A. S. Kurdyubov, I. Ya. Gerlovin, I. V. Ignatiev, Yu. P. Efimov, S. A. Eliseev, V. V. Petrov, Yu. K. Dolgikh, V. V. Ovsyankin, and A. V. Kavokin, *Phys. Rev. B* **91**, 115307 (2015).
- ²²J. Bellessa, C. Symonds, C. Meynaud, J. C. Plenet, E. Cambril, A. Miard, L. Ferlazzo, and A. Lemaître, *Phys. Rev. B* **78**, 205326 (2008).
- ²³B. Sermage, S. Long, I. Abram, J. Y. Marzin, J. Bloch, R. Paniel, and V. Thierry-Mieg, *Phys. Rev. B* **53**, 16516 (1996).
- ²⁴A. V. Trifonov, E. D. Cherotchenko, J. L. Carthy, I. V. Ignatiev, A. Tzimis, S. I. Tsintzos, Z. Hatzopoulos, P. G. Savvidis, and A. V. Kavokin, e-print [arXiv:1507.08870](https://arxiv.org/abs/1507.08870).